HeartRhythm

The Official Journal of the Heart Rhythm Society, The Cardiac Electrophysiology Society, and The Pediatric & Congenital Electrophysiology Society

Heart Rhythm Society SM

Enhancing transvenous lead extraction risk prediction: Integrating imaging biomarkers into machine learning models

Vishal S. Mehta, MBBS,[1,2] YingLiang Ma, PhD,[2,3] Nadeev Wijesuriya, MBBS,[1,2] Felicity DeVere, MBBS,[1,2] Sandra Howell, MBBS,[1,2] Mark K. Elliott, MBBS, PhD,[1,2] Nilanka N. Mannkakara, MBBS,[1,2] Tatiana Hamakarim,[1,2] Tom Wong, PhD, FHRS,[1,2,4] Hugh O'Brien, PhD,[2] Steven Niederer, DPhil,[2,4] Reza Razavi, PhD,[1,2] Christopher A. Rinaldi, MD, FHRS[1,2,5]

ABSTRACT

BACKGROUND Machine learning (ML) models have been proposed to predict risk related to transvenous lead extraction (TLE).

OBJECTIVE The purpose of this study was to test whether integrating imaging data into an existing ML model increases its ability to predict major adverse events (MAEs; procedure-related major complications and procedure-related deaths) and lengthy procedures ($\geq$100 minutes).

METHODS We hypothesized certain features—(1) lead angulation, (2) coil percentage inside the superior vena cava (SVC), and (3) number of overlapping leads in the SVC—detected from a pre-TLE plain anteroposterior chest radiograph (CXR) would improve prediction of MAE and long procedural times. A deep-learning convolutional neural network was developed to automatically detect these CXR features.

RESULTS A total of 1050 cases were included, with 24 MAEs (2.3%) . The neural network was able to detect (1) heart border with 100% accuracy; (2) coils with 98% accuracy; and (3) acute angle in the right ventricle and SVC with 91% and 70% accuracy, respectively. The following features significantly improved MAE prediction: (1) $\geq$50% coil within the SVC; (2) $\geq$2 overlapping leads in the SVC; and (3) acute lead angulation. Balanced accuracy (0.74–0.87), sensitivity (68%–83%), specificity (72%–91%), and area under the curve (AUC) (0.767–0.962) all improved with imaging biomarkers. Prediction of lengthy procedures also improved: balanced accuracy (0.76–0.86), sensitivity (75%–85%), specificity (63%–87%), and AUC (0.684–0.913).

CONCLUSION Risk prediction tools integrating imaging biomarkers significantly increases the ability of ML models to predict risk of MAE and long procedural time related to TLE.

KEYWORDS Transvenous lead extraction; Complications; Machine Learning; Artificial intelligence; Risk prediction; Computer vision

(Heart Rhythm 2024;■:1–10)

Introduction

The progressive rise of cardiac implantable electronic devices over the last 20 years has been mirrored by an increased requirement for lead extraction. Transvenous lead extraction (TLE) remains a safe procedure in the majority of cases, with the incidence of procedure-related major complications quoted as 1.6% in a systematic review of 18,433 patients.[1] Although procedural success is high, an increasing number of patients are at risk for adverse outcomes because of a high burden of comorbidities and multiple previous device interventions.[2] Improved risk stratification of patients based on likelihood of risk of adverse outcomes and procedural complexity is important for informed patient consent and appropriate resource allocation basis.[3]

From the [1]Cardiology Department, Guy's and St Thomas' NHS Foundation Trust, London, United Kingdom, [2]School of Biomedical Engineering and Imaging Sciences, King's College London, London, United Kingdom, [3]School of Computing Sciences, University of East Anglia, Norwich, United Kingdom, [4]National Heart and Lung Institute, Imperial College London, Hammersmith Hospital, London, United Kingdom, and [5]Heart Vascular & Thoracic Institute, Cleveland Clinic London, London, United Kingdom.

https://doi.org/10.1016/j.hrthm.2024.02.015

Table 1 Performance measures used to describe results of the neural network and machine learning model to predict MAE

Performance measure	Definition	Formula
Balanced accuracy	Balanced accuracy, rather than total accuracy, was utilized as the primary performance measure in view of the skewed distribution of outcomes with no MAEs vs those with MAEs, that is, there were very few cases involving MAEs in both datasets.[9] Using accuracy alone would overestimate the ability of the risk stratification method to appropriately identify the patient risk. Balanced accuracy is the mean accuracy for each class.	$\frac{TPR+TNR}{2}$
Precision	Precision is the ability of a model to identify only the relevant objects, that is, precision is how good the model is at accurately identifying a geometric feature.	$\frac{TP}{TP+FP}=\frac{TP}{\text{All detections}}$
Recall	Recall is the ability of a model to find all the relevant cases, that is, how many times the model was able to accurately identify a geometric feature.	$\frac{TP}{TP+FN}=\frac{TP}{\text{All ground truths}}$
F1 score	*F1* score is a method of calculating a mean of precision and recall.	$2 * \frac{\text{Precision} * \text{Recall}}{\text{Precision}+\text{Recall}}$
JSC	JSC is a statistical measure for correlating the similarity between binary data samples (defined as sample A and B). M_{11} represents the total number of attributes, where sample A and B both have a value of 1. M_{01} represents the total number of attributes where the attribute of A is 0 and the attribute of B is 1. M_{10} represents the total number of attributes where the attribute of A is 1 and the attribute of B is 0. It represents the percent of characteristics found in both samples and found in only 1 sample, that is, JSC of 0.3 means 30% of the characteristics were found in both samples, and 70% were found in only 1 of the 2 samples.	$JSC=\frac{M_{11}}{M_{01}+M_{10}+M_{11}}$

FN = false negative; FP = false positive; JSC = Jaccard similarity coefficient; MAE = major adverse event; TNR = true negative rate; TP = true positive; TPR = true positive rate.

Multiple risk scores have been developed; however, their predictive capability is constrained by the rarity of adverse events, the binary nature of preprocedural risk factors, and variation in methodology.[4,5] We previously published a risk assessment model to predict risk of adverse events using machine learning (ML) methods. The study used patient-level data derived from the European Society of Cardiology EORP (EURObservational Research Programme) ELECTRa (European Lead Extraction ConTRolled) registry of 3555 patients undergoing TLE in 73 centers across Europe.[6] The predictive capability of this ML model was tested against an independent registry of >1000 patients and its performance compared to an established clinical risk score—the ELECTRa Registry Outcome Score (EROS).[7]

We hypothesized that geometric features extracted from a preprocedure plain anteroposterior chest radiograph (CXR) would improve the predictive capability of this ML model. This study aimed to (1) develop a deep learning (DL)–based, convolutional neural network to automatically detect geometric features relevant to risk of TLE from preprocedure CXRs; (2) evaluate whether these features improve the previously published performance of this ML model; and (3) assess whether the same methods could predict long procedural times (which acted as a proxy for procedural complexity).

Abbreviations

AUC: area under the curve

CXR: chest radiograph

DL: deep learning

EROS: ELECTRa Registry Outcome Score

ICD: implantable cardioverter-defibrillator

JSC: Jaccard similarity coefficient

MAE: major adverse event

ML: machine learning

RV: right ventricle

SVC: superior vena cava

TLE: transvenous lead extraction

Methods

The database collection and analysis were approved by the Institutional Review Board of Guy's and St Thomas' Hospital.

Study populations and outcome definitions

A prospectively collected database of all consecutive patients undergoing TLE between October 2000 and November 2019 were recorded on a computer database at Guy's and St Thomas' NHS Foundation Trust, a high-volume UK TLE center used for CXR data. A total of 1171 patients underwent TLE during this period. The intended outcome from the ML model was preprocedural identification of patients at high risk for negative outcomes and complex procedures. The outcome of major adverse event (MAE)—defined as a composite of procedure-related major complication and procedure-related death—was selected as the ground truth to capture this goal. These were defined in both datasets by the consensus statement in the ELECTRa dataset[3,8] (Supplemental Table 1). Each MAE was counted only

Table 2 Baseline characteristics of all subjects in test dataset (N = 1050)

Demographics	
Male	772 (73.5)
Explant age (y)	65.30 ± 14.49
Device type	
Single-chamber PPM	74 (7.1)
Dual-chamber PPM	370 (35.3)
Implantable cardioverter-defibrillator	297 (28.3)
CRT-pacemaker	67 (6.4)
CRT-defibrillator	240 (22.9)
Leads	
Dwell time (y)	5.30 [1.80–10.00]
Active RV lead	546 (24.4)
Passive RV lead	207 (19.7)
Active RA lead	534 (50.9)
Passive RA lead	201 (19.1)
LV lead	234 (22.3)
Single-coil defibrillator lead	224 (21.3)
Dual-coil defibrillator lead	219 (20.9)
Total no. of leads extracted	
1	294 (28.0)
2	444 (42.3)
3	216 (20.6)
≥4	96 (9.1)
Side of explant	
Left-sided	856 (81.5)
Right-sided	131 (12.5)
Both sides	63 (6.0)
Extraction indication	
Noninfective indication	482 (45.9)
Local infection	372 (35.5)
Systemic infection	196 (18.7)
Extraction history	
History of previous extraction	118 (11.2)
Comorbidities	
IHD	402 (39.6)
Valvular disease	100 (9.9)
Heart failure	414 (40.7)
Diabetes mellitus	174 (17.3)
Hypertension	406 (40.4)
Respiratory disease	145 (14.4)
CKD	206 (20.1)
ESRF	10 (1.0)
Cardiac function	
LVEF (%)	44.77 ± 14.34
Biochemistry	
Creatinine (μmol/L)	92.00 [77.00–119.25]
eGFR (mL/min/1.73 m^2)	67.47 ± 20.75
eGFR <60 mL/min/1.73 m^2	391 (37.2)
Peak CRP (mg/L)	6.00 [2.00–18.00]

Values are given as n (%), mean ± SD, or median [interquartile range].
CKD = chronic kidney disease; CRP = C-reactive protein; CRT = cardiac resynchronization therapy; eGFR = estimated glomerular filtration rate; ESRF = end-stage renal failure; IHD = ischemic heart disease; LV = left ventricle; LVEF = left ventricular ejection fraction; PPM = permanent pacemaker; RA = right atrium; RV = right ventricle.

once per patient (ie, if a major complication and death were recorded for the same patient, this was counted as only 1 MAE). Prolonged procedural time was defined as time taken from procedure start to removal of targeted leads lasting >100 minutes. This cutoff was chosen because it was the 75th percentile of procedural duration (ie, 25% of the cases were >100 minutes).

Statistical analysis

Categorical variables were compared with the χ^2 test or Fisher exact test. Normally distributed data were analyzed using the independent samples *t* test. Non-normally distributed continuous data were analyzed using the Kruskal-Wallis 1-way analysis of variance test. Results are given as mean ± SD for normally distributed variables and as median [interquartile range] for non-normally distributed variables. Categorical variables are given as number of patients (% of group). These analyses were performed using R Version 1.3.1093 (R Foundation for Statistical Computing, Vienna, Austria).

The definitions of the performance measures used to describe the accuracy of the neural network to detect the geometric features and the ML model to predict MAE are described in Table 1. The Jaccard similarity coefficient (JSC) was used as a simple statistical measure for testing the correlation between an identified individual geometric feature on CXR and the binary outcome of MAE.[10] Because the dataset is known to be imbalanced,[6] an adaptive synthetic sampling technique was used to balance the datasets and calculate the JSC.[11] The relative importance of each feature in the final model is represented by an *F* score, which is a way to rank the features based on their contribution to the final prediction, that is, the higher the *F* score, the greater that particular feature contributes to the model's prediction of risk. The *F* score for each feature should be considered in relation to the score of other features contributing to the model. Balanced accuracy, sensitivity, specificity, and receiver operating characteristic curves were used to assess the predictive capability of the ML model.

Overview of original ML study

We previously published an ML-based risk stratification tool trained using the ELECTRa Registry to predict the risk of MAEs in 3555 patients undergoing TLE and tested this on an independent registry of 1171 patients.[6] ML models were developed, including a self-normalizing neural network, stepwise logistic regression ("stepwise model"), support vector machines, and random forest model. These were compared to the EROS for MAEs.[3] ML techniques were similar to EROS by balanced accuracy (ML model 0.74 vs EROS 0.70) and superior by area under the curve (ML model 0.764 vs EROS 0.677). An improvement in accuracy was incremental, and it was hypothesized that integrating imaging biomarkers into this model would improve its predictive capability.

Rationale for radiograph feature selection

A combination of known risk factors and senior clinical opinion was considered when choosing appropriate features from a plain CXR. In previously published data, the presence of an implantable cardioverter-defibrillator (ICD) lead, an increased number of leads extracted,[3,12] and likelihood of lead encapsulation[13] are established risk factors that could be detected from a plain CXR. The most common cause of procedure-related major complication or death is a tear in the superior vena cava (SVC),[14] so identifying accurate proxies for a model of the SVC and the location of leads and coils

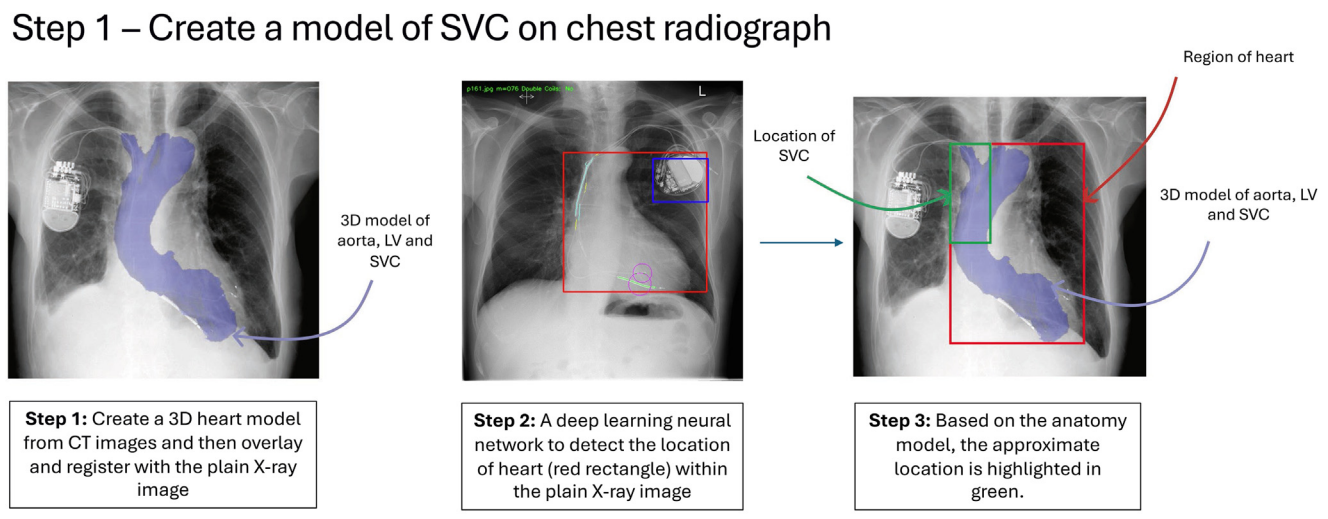

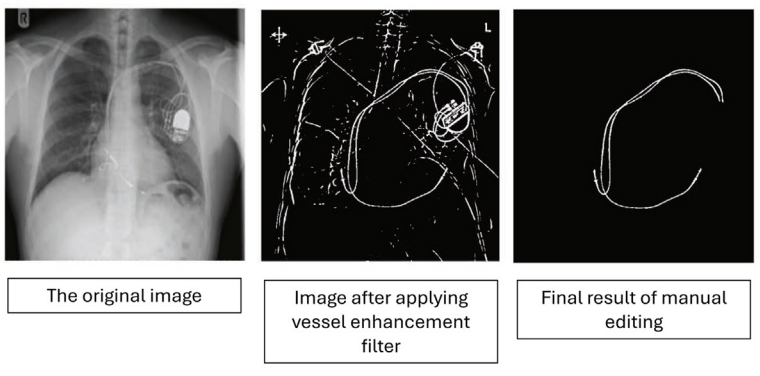

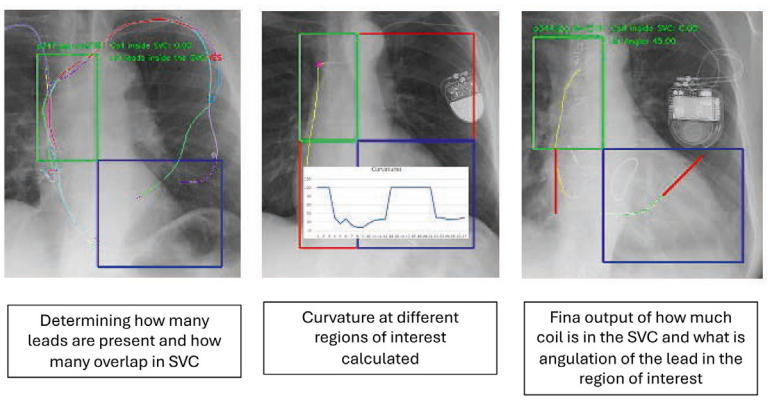

Figure 1
Overview of the deep learning framework to identify geometric features on a plain anteroposterior chest radiograph. 3D = 3-dimensional; CT = computed tomography; SVC = superior vena cava.

in relation to this was considered essential. It was also hypothesized that lead-to-lead interaction (measured by whether the leads were overlapping) and an acute (ie, <90°) angulation of the lead within the SVC or the myocardium were important factors to consider. An acute angle was defined as an angle between 0° and 90° of the lead itself at the locations of the SVC or the right ventricle (RV) (Supplemental Figure 1).

Table 3 Performance of the neural network in detecting the feature on CXR in comparison to the ground truth

Geometric feature	Accuracy	Precision	Recall	*F1* score
Detection of heart border*	NA	0.818	1	NA
Detection of coils	0.98	0.98	0.99	0.98
Detection of leads	0.782	0.879	0.836	0.857
Detect acute angle in SVC	0.7	0.833	0.714	0.769
Detect acute angle in RV	0.905	0.969	0.923	0.945

CXR = chest radiograph; RV = right ventricle; SVC = superior vena cava.
*Ability to detect >75% of the true heart border.

These geometric features were combined with the baseline characteristics of the patients to feed into an ML model to predict risk of MAE (Table 2). The model was based on the preprocedural features in a previously published ML model trained on the ELECTRa Registry and tested on the Guy's and St Thomas' Trust database.[6] All features considered and included in the final ML models, including and excluding geometric features, are given in Supplemental Table 2. An XGBoost classifier was chosen because of its high performance with imbalanced datasets and binary classifications, and is an ensemble learning method that combines the predictions of multiple models to produce a stronger prediction.[15] Due to the relative infrequency of MAEs observed, leave-one-out cross-validation was used.[16] For comparison, the added value of the geometric features was tested against the model using only the preprocedural characteristics listed in Table 2 (ie, excluding the geometric features from the CXR).

Overview of imaging biomarker detection framework

The DL framework to automatically identify the geometric features has been previously described in detail.[17] A summary of the process is illustrated in Figure 1 and outlined in the following.

Identification of the approximate location of the SVC

The SVC is not readily identifiable on CXR unless contrast is injected; however, it is possible to determine an approximate course in relation to heart anatomy. Using known common approximate models of heart anatomy, we were able to approximate the location of the SVC. The location of the SVC is approximately half the height and one-third of the width of the heart region (Supplemental figure 2). This was validated by overlaying 3-dimensional anatomy models extracted from 20 preprocedural computed tomographic scans. In order to use this automated SVC location on CXR, the heart region must be detected. A transfer learning approach was used to detect the heart region that was based on a modified VGG16 model. Seventy percent of the CXRs were used for training and 30% for accuracy testing.

Detection of lead and coils

To segment the leads and coils from the CXRs, a U-Net convolutional network was trained and tested on the CXR dataset. To semi-automate this process, a vessel enhancement filter[18] was used to extract all wirelike objects, and the resultant image was automatically binarized. An experienced clinician manually removed features not leads or coils, which acted as the "ground truth" for the U-net model to train on 737 CXRs to automatically extract coils and leads while ignoring other objects such as electrocardiographic leads, ribs, and the generator. To improve detection with poor-quality images, the contrast or brightness of these images was reduced by a factor between 0.6 and 0.9 to create an additional 1474 training images.

Table 4 Geometric feature detected and respective JSC

Geometric feature	JSC
50% of coil and ≥2 overlapping leads inside the SVC	0.35
Acute angle in the RV	0.03
Acute angle near entry point of the SVC	0.01

JSC = Jaccard similarity coefficient; RV = right ventricle; SVC = superior vena cava.

Extracting geometric features

A centerline extraction method was used to precisely identify the lead or coil detected that was present in the SVC.[19] In this process, a binarized image of the detected coils and leads was skeletonized and a 1-pixel wide object created. A contour-finding algorithm and wire reconstruction method were used to determine the course of the lead, compute the location and angulation of the leads or coil, and determine whether they were overlapping.[20,21] The 2 points of angulation interest were at the point of entry into the SVC or within the RV (Supplemental Figure 1). The ground truth was the manual labeling of all angles of the leads in 2 positions: (1) entry point of the SVC and (2) inside the RV. Overlapping leads were defined as the centerlines of the leads overlapping with each other at least once.

Results

Baseline characteristics

The overall cohort included 1151 patients, of whom 1050 had preprocedure CXRs available for use in the current analysis (Table 2). There were 24 MAEs (2.3%), and the most common major complication was cardiac avulsion (n = 12 [1.2%]) (Supplemental Table 3). In total, there were 484 cases with complete procedural duration data available; of these, 123 (25.4%) had a long procedural time. Overall, 73.5% (n = 772) were male (mean age at explant 65.3 ± 14.5 years; mean left ventricular ejection fraction 44.8% ± 14.3%). Median lead dwell time was 5.30 [1.80–10.00] years, and the plurality of devices explanted were dual-chamber pacemakers (n = 370 [35.3%]) followed by ICDs (n = 297 [28.3%]). In total, 2246 leads were explanted, with a mean of 2.14 leads per procedure. A total of 443 defibrillator leads were explanted, of which 219 (49.4%) were dual-coil leads. The majority of extractions were for infective indications (n = 562 [54.1%]), with

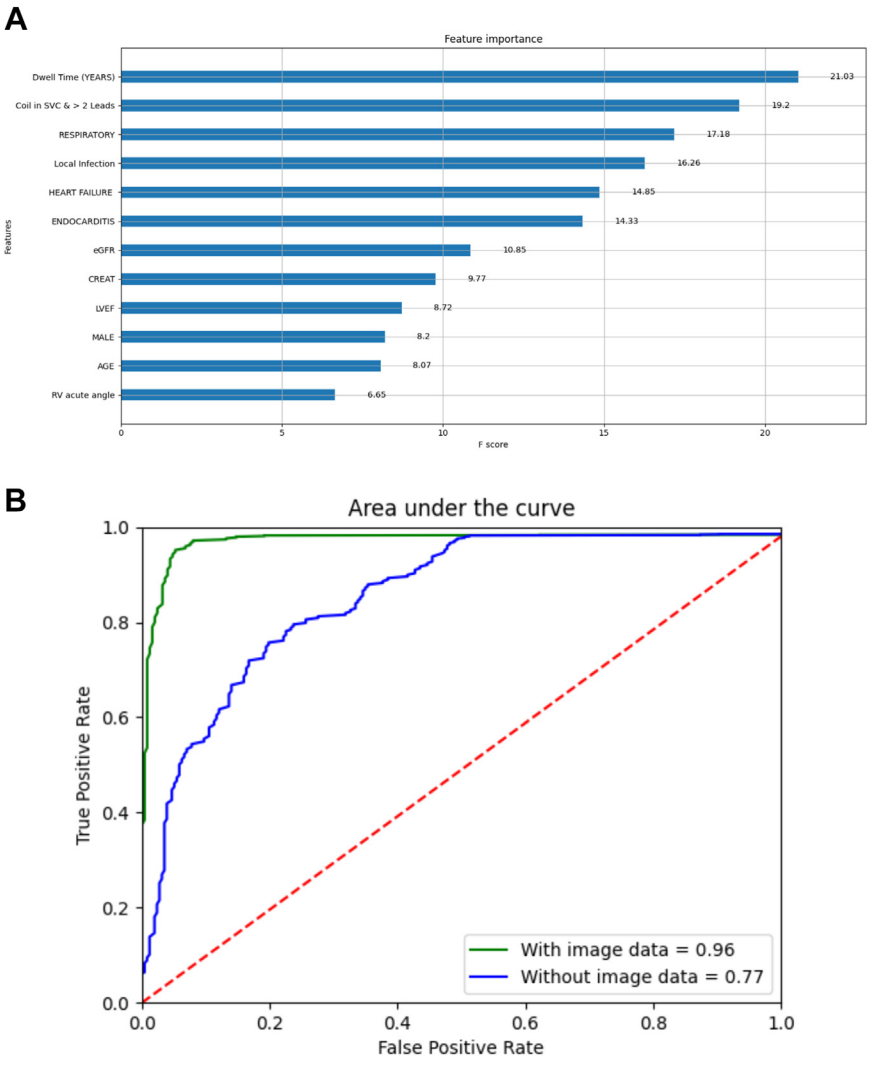

Figure 2
Machine learning (ML) model for predicting major adverse event (MAE). **A:** Features and their respective weights for predicting MAE. **B:** Receiver operating characteristic (ROC) curve of the ML model for predicting MAE. *Blue* shows ROC curve using a model without imaging data. *Green* shows the ROC curve using a model with imaging.

most for local infections (n = 372 [52.6%]). The most common comorbidities were heart failure (n = 414 [40.7%]) and hypertension (n = 406 [40.4%]). In total, 206 patients (20.1%) had CKD, with a median baseline creatinine of 92.00 [77–119.3] μmol/L.

Automated detection performance

The performance of the DL neural network in automatically detecting the geometric features is given in Table 3. It was excellent in all areas except for acute angle detection in the SVC.

Geometric feature selection and DL model for risk assessment

The geometric features assessed and their respective JSC values are given in Table 4. A total of 143 cases had an acute angle in the RV. Greater than 50% of a coil in the SVC combined with ≥2 overlapping leads in the SVC had a highly sensitive JSC value and resulted in much better performance and contribution overall to the model in predicting MAE rather than separating the features (Supplemental Table 4). Therefore, the following geometric features were included in the final model: (1) >50% coil in the SVC and ≥2 overlapping leads in the SVC; and (2) acute angle in the RV.

Ability of model to predict MAE and long procedural time

The most important features in the model excluding geometric features are dwell time, left ventricular ejection fraction, and estimated glomerular filtration rate (Supplemental Figure 3) for predicting MAE. The presence of a dual-coil lead was only the 10th most important feature in the model excluding geometric features. In comparison, 2 geometric features were the 2nd and 12th most important features in the model including the CXR data (Figure 2A). The most important

Table 5 Predictive capability of the machine learning model to predict a major adverse event or long procedure excluding and including the geometric features from the preprocedural chest radiograph

Outcome	Results	Balanced accuracy	Specificity	Sensitivity	Area under curve
Major adverse event	Excluding imaging	0.74	0.63	0.62	0.77
	Including imaging	0.87	0.91	0.83	0.96
Long procedural time	Excluding imaging	0.76	0.63	0.75	0.684
	Including imaging	0.86	0.87	0.85	0.913

preprocedural clinical factor remained lead dwell time; however, the presence of ≥50% of a coil in the SVC and ≥2 overlapping leads had a similar predictive value for MAE as dwell time (*F* score 19.7 vs 18.7). An acute angle in the RV was almost as important as left ventricular ejection fraction (*F* score 7.16 vs 8.53) and more important than male gender (*F* score 7.07). Infective factors were of high relevance (endocarditis *F* score 16.85; local infective indication *F* score 15.21).

There was a significant improvement in the ability of the model to predict MAE with CXR data (Table 5). Balanced accuracy improved from 0.75 to 0.87, sensitivity improved from 69% to 83%, specificity improved from 72% to 91%, and area under the curve (AUC) improved from 0.767 to 0.962 (Figure 2B). There was no significant difference in model performance when using the ground truth data compared to automated CXR feature detection (Supplemental Figure 4).

With respect to long procedural time, the most important preprocedural clinical factors were endocarditis (*F* score 12.95), respiratory disease (*F* score 11.77), and local infection (*F* score 7.01) (Figure 3A). The most predictive feature was >50% of coil in the SVC and ≥2 overlapping leads from the preprocedural CXR of (*F* score 48.11). Balanced accuracy improved from 0.76 to 0.86, sensitivity improved from 75% to 87%, specificity improved from 63% to 85%, and AUC improved from 0.684 to 0.913 (Figure 3B).

We explored whether inclusion of lateral CXRs increased the predictive capability of the model; however, there was no significant improvement, with balanced accuracy increasing from 0.91 to 0.92 and AUC from 0.962 to 0.969 (Supplemental Appendix).

Discussion

This is the first DL-derived model integrating imaging biomarkers to predict risk following TLE. The main findings are as follows. (1) Convolutional neural networks can automatically, and accurately, detect key geometric features relevant to lead extraction, particularly the SVC location, the course of a lead, lead angulation, percentage of coil in the SVC, and whether leads overlap. (2) Imaging biomarkers integrated into an independently tested ML model significantly improved its predictive capability. (3) ML can improve prediction of potentially lengthy procedures.

Relevance of risk stratification

Undertaking a lead extraction procedure with the appropriate expertise and tools and in the correct setting is one of the cornerstones of reducing procedural risk. Extensive data have shown that high-volume lead extraction centers perform better compared with low-volume centers and that patients with known risk factors who have undergone lead extraction in a low-volume center have poorer outcomes, reinforcing the fact that high-volume operators should perform higher-risk procedures.[1,22] TLE is a resource-intensive, expensive procedure, which often is poorly reimbursed relative to their economic costs to the health institution.[23] Within this context, risk stratification scores are a helpful tool for the heart team when triaging patients appropriately preprocedure.

Several risk stratification tools, primarily using a combination of expert consensus and logistic analysis, have been published. Bontempi et al[24] developed the "LED risk score," which identified the number of extracted leads within a procedure, lead age, dual-coil lead, and presence of vegetation as increasing the likelihood of a complex procedure. Kancharla et al[4] derived a risk score including ICD lead >5 years old and pacemaker lead >10 years old. The tool was prospectively validated on whether patients should have TLE performed in an operating room or device laboratory. The EROS score developed by Sidhu et al[7] categorized patients as low (EROS 1), intermediate (EROS 2), and high risk (EROS 3). EROS 3 risk was heavily dependent on lead dwell time: pacemaker lead >15 years and ICD lead >10 years from implant. We previously compared the EROS score to an ML-based risk score trained on the ELECTRa database and tested on the dataset used in this study with AUC of 0.764; however, the study concluded that more nuanced and richer preprocedural data were required to make ML a beneficial tool.[6] This current study has built on that conclusion and shown that features extracted from a plain CXR—a simple investigation that should be performed in all patients undergoing lead extraction—significantly improves risk prediction. This is particularly marked in the geometric features related to the SVC and the congestion of leads within it. TLE has a high procedural success rate and complications remain low, so an excellent AUC is necessary to provide the necessary sensitivity and specificity for added value. AUC improvement from 0.76 to 0.96 in this study demonstrates such an improvement. AUC score between 0.9 and 0.99 is considered excellent.[25]

Clinical perspectives

Better risk stratification tools have the potential to ensure stronger mitigation and minimize the risk of MAE. The value of such a risk tool may be useful for both infective and noninfective indications of lead extraction. For infective indication,

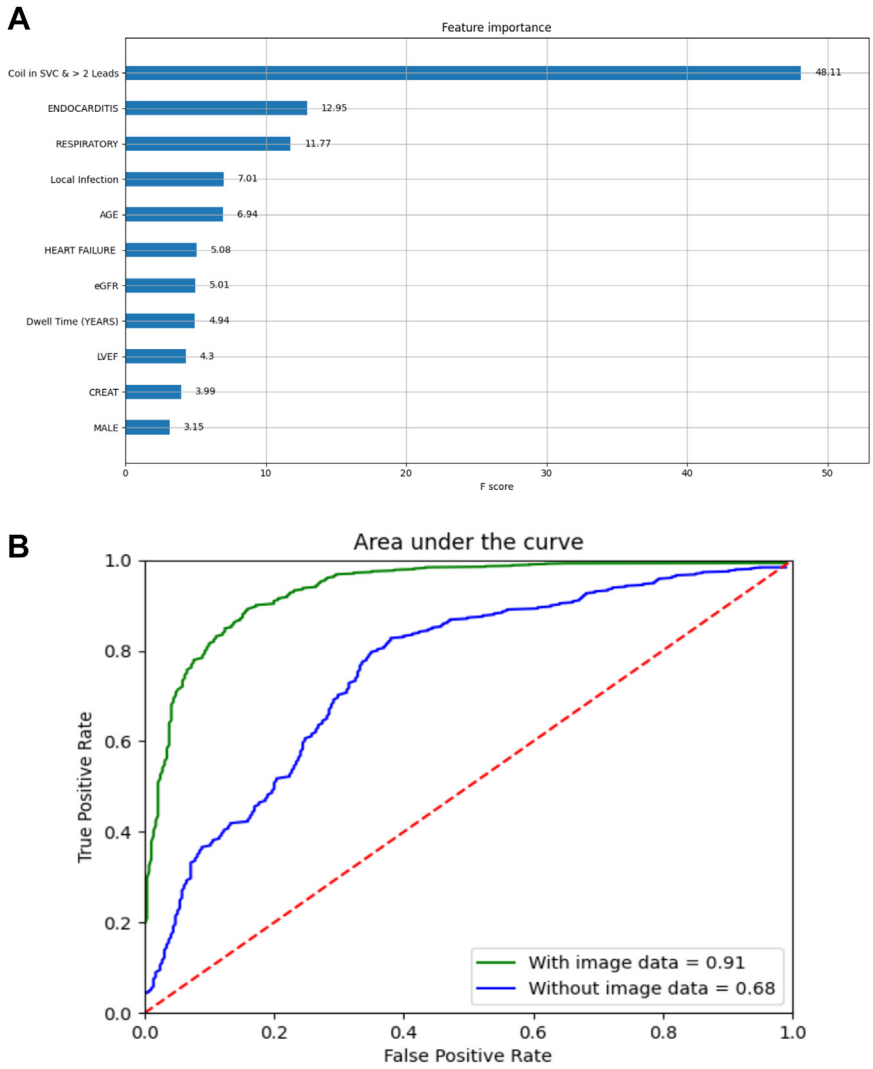

Figure 3
ML model for predicting long procedural times. **A:** Features and their respective weights for predicting MAE. **B:** ROC curve of the ML model for predicting MAE. Blue shows the ROC curve using a model without imaging data. Green shows the ROC curve using a model with imaging. Abbreviations as in Figure 2.

there is always a class I indication to extract infected material[26]; however, who is likely to be at significantly higher risk of an adverse event is not always clear. For noninfective indications, the evidence for lead extraction is less strong, with clinical consensus and patient preference primarily determining whether a malfunctioning lead should be extracted or left redundant when a new lead is implanted. Currently, the data regarding the potential harms of abandoning leads in such circumstances are unclear, and weighing benefits and risks is a largely a joint decision between the cardiologist and the patient.[27] Having a highly sensitive and specific test would help quantify that risk better and allow more objective decision-making. The current study provides the framework for such a test.

In addition, the ability of the current model to determine those at higher risk for a long procedural times has clinical utility. Traditional risk factors for complex procedures, particularly the presence of an ICD, markers of infection, and respiratory disease, were strong influencers in the model. These patients likely had more complex general anesthetic requirements in view of their endocarditis and respiratory disease, and the presence of a coil increased the number of tools and time required to extract the material. These factors are important when determining resource and time allocation, and whether the procedure should occur in the operating room, or hybrid or device laboratory.

Future perspectives

A previous study by Howard et al[28] showed the utility of neural networks to accurately identified the model of pacemakers and defibrillators; however, this is the first DL framework to automatically detect CXR and lead-related features that increase the risk of MAE following TLE. We demonstrated that novel methods can improve the prediction of an adverse outcome by integrating a ubiquitous and inexpensive investigation, such as CXR. All patients should have CXR pre-TLE, and these data, combined with baseline clinical features,

can be routinely integrated into preprocedural planning. Such techniques potentially also can be used in cross-sectional imaging, which has greater spatial resolution of the 3-dimensional course of a lead and coil, particularly in relation to the SVC. However, contrast-enhanced computed tomographic imaging using current DL techniques is challenging because of the high intensity of artifacts from the lead and coils. Real-time fluoroscopy and motion tracking could give added information on lead-to-lead or lead-to-SVC interaction, providing a far greater understanding of how lead kinetics affect procedural risk.[21]

Overall, the whole process is computationally inexpensive. The computer vision algorithm works within 500 ms to identify the coil and lead route, as well calculate the angles. The prediction algorithm (XGBoost) performs the prediction in 1000 ms to produce the prediction once the relevant baseline demographic and imaging data are uploaded. We anticipate that this tool can be used before or during the "heart team" meeting, at which a decision is made on the appropriateness and location of any lead extraction procedure.

Study limitations

The high imbalance between MAE (2.4%) and non-MAE (97.6%) cases means much larger datasets are required to increase the confidence in our results. To mitigate this, leave-one-out validation and ML algorithms (ie, XG Boost and adaptive synthetic sampling technique), which perform well with imbalanced data, were used. Certain low-frequency but traditional high-risk features of patients undergoing TLE, such as lead calcification, were not included in the analysis because they were not consistently recorded. The risk prediction model was applied retrospectively, which may introduce bias, and a prospective validation study would mitigate this. Although the neural network to detect most geometric features was robust, it was suboptimal in detecting acute angles in the SVC due to the low frequency of such cases; therefore, this feature was not included in the final model. A plain anteroposterior CXR was used; however, for 3-dimensional distances between individual leads, a higher volume of lateral CXRs may be included in future analyses.

Conclusion

This is the first study to use imaging biomarkers to assess risk related to TLE. We have developed a high-performing automated DL algorithm to accurately extract geometric features from a plain anterior posterior CXR. By integrating this imaging data to an existing ML model, we have significantly improved the prediction of adverse events and potentially complex procedures related to TLE.

Appendix

Supplementary data

Supplementary data associated with this article can be found in the online version at https://doi.org/10.1016/j.hrthm.2024.02.015.

Funding Sources: The authors are supported by the Wellcome/EPSRC Centre for Medical Engineering (WT203148/Z/16/Z).

Disclosures: Dr Wijesuriya receives fellowship funding from the British Heart Foundation (FS/CRTF/22/24362). Dr Mehta has received fellowship funding from Siemens and Abbott. Dr Mannkakara is in receipt of fellowship funding from Heart Research UK (Grant No. RG2701) and Abbott. Dr Ma receives research funding from UK Engineering and Physical Sciences Research Council (EP/X023826/1). Dr Niederer acknowledges support from the UK Engineering and Physical Sciences Research Council (EP/M012492/1, NS/A000049/1, and EP/P01268X/1); British Heart Foundation (PG/15/91/31812, PG/13/37/30280, SP/18/6/33805); US National Institutes of Health (NIH R01-HL152256); European Research Council (ERC PREDICT-HF 864055); and Kings Health Partners London National Institute for Health Research (NIHR) Biomedical Research Centre. Dr Rinaldi receives research funding and/or consultation fees from Abbott, Medtronic, Boston Scientific, Spectranetics, and MicroPort outside of the submitted work. All other authors have no conflicts of interest to disclose.

Authorship: All authors attest they meet the current ICMJE criteria for authorship.

Address reprint requests and correspondence: Dr Vishal Mehta, School of Biomedical Engineering and Imaging Sciences, St Thomas' Hospital, Rayne Institute, 4th Floor Lamberth Wing, London SE1 7EH, United Kingdom. E-mail address: vishal.mehta@kcl.ac.uk

References

1. Pelargonio G, Narducci ML, Manzoli L, et al. Safety of transvenous lead extraction according to centre volume: a systematic review and meta-analysis. Europace 2014;16:1496–1507.
2. Mehta VS, Elliott MK, Sidhu BS, et al. Long-term survival following transvenous lead extraction: importance of indication and comorbidities. Heart Rhythm 2021;18:1566–1576.
3. Bongiorni MG, Kennergren C, Butter C, et al. The European Lead Extraction ConTRolled (ELECTRa) study: a European Heart Rhythm Association (EHRA) Registry of transvenous lead extraction outcomes. Eur Heart J 2017;38:2995–3005.
4. Kancharla K, Acker NG, Li Z, et al. Efficacy and safety of transvenous lead extraction in the device laboratory and operating room guided by a novel risk stratification scheme. JACC Clin Electrophysiol 2019;5:174–182.
5. Jacheć W, Polewczyk A, Polewczyk M, Tomasik A, Kutarski A. Transvenous lead extraction SAFeTY score for risk stratification and proper patient selection for removal procedures using mechanical tools. J Clin Med 2020;9:361.
6. Mehta VS, O'Brien H, Elliott MK, et al. Machine learning–derived major adverse event prediction of patients undergoing transvenous lead extraction: using the ESC EHRA EORP European lead extraction ConTRolled ELECTRa registry. Heart Rhythm 2022;19:885–893.
7. Sidhu BS, Ayis S, Gould J, et al. Risk stratification of patients undergoing transvenous lead extraction with the ELECTRa Registry Outcome Score (EROS): an ESC EHRA EORP European lead extraction ConTRolled ELECTRa registry analysis. Europace 2021;23:1462–1471.
8. Maytin M, Jones SO, Epstein LM. Long-term mortality after transvenous lead extraction. Circ Arrhythm Electrophysiol 2012;5:252–257.
9. García V, Mollineda RA, Sánchez JS. Index of balanced accuracy: a performance measure for skewed class distributions. 2009. 5524 LNCS. Lecture Notes in Computer Science (including subseries Lecture Notes in Artificial Intelligence and Lecture Notes in Bioinformatics) 2009;441–448.
10. Chung NC, Miasojedow BZ, Startek M, Gambin A. Jaccard/Tanimoto similarity test and estimation methods for biological presence-absence data. BMC Bioinformatics 2019;20(Suppl 15):644.
11. Institute of Electrical and Electronics Engineers: Neural Networks, 2008. IJCNN 2008. IEEE World Congress on Computational Intelligence, IEEE International Joint Conference. June 1–8, 2008.
12. Segreti L, Rinaldi CA, Claridge S, et al. Procedural outcomes associated with transvenous lead extraction in patients with abandoned leads: an ESC-EHRA ELECTRa (European Lead Extraction ConTRolled) Registry Sub-Analysis. Europace 2019;21:645–654.

13. Kołodzińska A, Kutarski A, Koperski Ł, Grabowski M, Małecka B, Opolski G. Differences in encapsulating lead tissue in patients who underwent transvenous lead removal. Europace 2012;14:994–1001.
14. Tułecki Ł, Polewczyk A, Jacheć W, et al. A study of major and minor complications of 1500 transvenous lead extraction procedures performed with optimal safety at two high-volume referral centers. Int J Environ Res Public Health 2021;18:10416.
15. Chen T, Guestrin C. XGBoost: A Scalable Tree Boosting System. 2016. http://arxiv.org/abs/1603.02754.
16. Sengupta PP, Shrestha S, Berthon B, et al. Proposed Requirements for Cardiovascular Imaging-Related Machine Learning Evaluation (PRIME): a checklist: reviewed by the American College of Cardiology Healthcare Innovation Council. JACC Cardiovasc Imaging 2020;13:2017–2035.
17. Ma Y, Mehta VS, Rinaldi CA, Hu P, Niederer S, Razavi R. Automatic detection of coil position in the chest X-ray images for assessing the risks of lead extraction procedures. 2023. June 16. In: Bernard O, Clarysse P, Duchateau N, Ohayon J, Viallon M, eds. Functional Imaging and Modeling of the Heart. FIMH 2023. Lecture Notes in Computer Science. Cham: Springer; 2023. https://doi.org/10.1007/978-3-031-35302-4_32. Volume 13958.
18. Frangi AF, Niessen WJ, Vincken KL, Viergever MA. Multiscale vessel enhancement filtering. In: Wells WM, Colchester A, Delp S, eds. Medical Image Computing and Computer-Assisted Intervention—MICCAI'98 Berlin. Heidelberg. Berlin Heidelberg: Springer; 1998. p. 130–137.
19. Ma YL, Alhrishy M, Narayan SA, Mountney P, Rhode KS. A novel real-time computational framework for detecting catheters and rigid guidewires in cardiac catheterization procedures. Med Phys 2018;45:5066–5079.
20. Suzuki S, be K. Topological structural analysis of digitized binary images by border following. Comput Vis Graph Image Process 1985;30:32–46.
21. Ma Y, Zhou D, Ye L, Housden RJ, Fazili A, Rhode KS. A tensor-based catheter and wire detection and tracking framework and its clinical applications. IEEE Trans Biomed Eng 2022;69:635–644.
22. Sidhu BS, Gould J, Bunce C, et al. The effect of centre volume and procedure location on major complications and mortality from transvenous lead extraction: an ESC EHRA EORP European Lead Extraction ConTRolled ELECTRa registry subanalysis. Europace 2020;22:1718–1728.
23. Gould J, Sidhu BS, Porter B, et al. Financial and resource costs of transvenous lead extraction in a high-volume lead extraction centre. Heart 2020;1:931–937.
24. Bontempi L, Vassanelli F, Cerini M, et al. Predicting the difficulty of a lead extraction procedure: The tED index. J Cardiovasc Med 2014;15:668–673.
25. Carter JV, Pan J, Rai SN, Galandiuk S. ROC-ing along: evaluation and interpretation of receiver operating characteristic curves. Surgery 2016;159:1638–1645.
26. Kusumoto FM, Schoenfeld MH, Wilkoff BL, et al. 2017 HRS expert consensus statement on cardiovascular implantable electronic device lead management and extraction. Heart Rhythm 2017;14:e503–e551.
27. Poole JE, Gleva MJ, Mela T, et al. Complication rates associated with pacemaker or implantable cardioverter-defibrillator generator replacements and upgrade procedures: results from the REPLACE registry. Circulation 2010;122:1553–1561.
28. Howard JP, Fisher L, Shun-Shin MJ, et al. Cardiac rhythm device identification using neural networks. JACC Clin Electrophysiol 2019;5:576–586.